July 2018

Integrated Control of Multi-Zone Buildings with Ventilation and VRF systems in Cooling Mode

Christopher R. Laughman
Mitsubishi Electric Research Laboratories, United States of America, laughman@merl.com

Hongtao Qiao
Mitsubishi Electric Research Laboratories, United States of America, qiao@merl.com

Scott A. Bortoff
Mitsubishi Electric Research Laboratories, United States of America, bortoff@merl.com

Integrated Control of Multi-Zone Buildings with Ventilation and VRF systems in Cooling Mode

Christopher R. Laughman*, Scott A. Bortoff, Hongtao Qiao

Mitsubishi Electric Research Laboratories
Cambridge, MA, USA
{laughman,bortoff,qiao}@merl.com

* Corresponding Author

ABSTRACT

One common strategy for achieving reduced energy consumption and improved comfort in modern high-performance buildings involves the use of multiple interacting heating, cooling, and ventilation systems. Because tighter and more insulating building envelopes are often accompanied by a reduction in the capacity of the space conditioning systems, the limited control authority of these smaller systems raises the importance of understanding dynamics and control in this built environment. This paper explores the use of model-based strategies for analyzing and controlling the behavior of a representative building incorporating both a multi-zone VRF system and a ventilation system. The Modelica language facilitates the use of rapid prototyping and trade studies with three different ventilation systems - a fan-only system, an ERV system, and a DOAS - as well as the study of the performance of the building with each of these systems operating under closed-loop control. Analysis of the integrated system indicates that the subsystems interact dynamically, and that these dynamics must be considered during the design process. These three systems are evaluated over a 2 days of operation with realistic solar and weather inputs, and the DOAS system is found to consume 27% less energy than the fan-only system and 16% less energy than the ERV system over that time interval.

1. INTRODUCTION

As researchers and policymakers continue to study the interactions of buildings with both their occupants and their surrounding environment, a number of trends have emerged that will govern future directions of development for the building industry. Perhaps the most recognizable of these trends is an increased interest in near-zero energy buildings that is driven by a variety of factors, including concerns about climate change, the impact of buildings on their local environment, and the perpetual pursuit of reduced operational cost. Ongoing work in understanding thermal comfort in occupied spaces has also demonstrated that additional measures beyond the sole regulation of sensible room temperature are needed to ensure that occupied spaces are comfortable. Furthermore, recent indoor air quality research provides ample evidence of the important health effects associated with the supply of a sufficient volume of fresh air to occupied spaces.

While these advanced performance objectives can potentially be achieved with a variety of approaches, including the construction of tighter buildings and the increased use of radiant heating and cooling systems, many of these different approaches share common characteristics. One common theme is that buildings will require a diversity of space conditioning systems, such as a combination of radiant and convective space conditioning systems, as well as separate ventilation systems, because the individual systems cannot independently satisfy all of the objectives. Lower loads in buildings due to advanced facade construction and reduced air leakage will also dictate the use of HVAC systems with lower heating and cooling capacities, resulting in systems that have reduced control authority over temperatures or humidities of concern. More variation in site-specific system architectures will also become common as architects and engineers collaborate to adapt building construction, system selection, and operation to local conditions in pursuit of the maximum performance.

Rigorous system-level design and control will be needed to achieve the theoretical performance benefits of these heterogeneous system combinations because the individual subsystems interact dynamically in the occupied space. For

example, the thermal conditions in a space with both convective space conditioning and ventilation systems will be affected by the coupled behavior of both systems, and poorly specified or controlled systems may result in excess energy consumption and/or poor regulation of comfort conditions. Constraints on the operation of these system combinations must also be managed to ensure that building-level operational requirements are met, such as minimum outdoor air flow rates, as well as satisfying manufacturer requirements and constraints for individual subsystems. These concerns are amplified in the case of multi-zone systems, as the interactions between terminal units within a given system amd between systems must be considered when designing the overall system architecture and controls.

Due to the excessive expense, significant time, and general impracticality of using experimentally-based processes to design system architectures and control algorithms for advanced buildings, model-based methodologies will be essential when performing trade studies for system and controls design. More pronounced interactions between the building structure and the HVAC systems will necessitate the use of an iterative approach to building design as architects, mechanical engineers, and energy consultants seek to achieve their performance and cost goals, and dynamic models will be a valuable tool for understanding the effect of their decisions on the occupant experience. Control system design will also be heavily reliant upon the proper use of models because space conditioning systems tend to be nonlinear and have time constants spanning many orders of magnitude, making the control design space difficult to explore experimentally.

A variety of work has been previously done to study and control the interactions between multiple space-conditioning systems in a multi-zone setting. Karunakaran et al. (2010) developed a set of fuzzy control laws to implement different ventilation strategies for regulating the combined behavior of a variable refrigerant flow (VRF) system and a variable air volume (VAV) system supplying fresh air to 2 zones, and experimental results on this controlled system yielded energy savings of 44% to 63% per day. Zhu et al. (2015) developed a control method based on optimal setpoints identified by a genetic algorithm to regulate the behavior of a combined VRF and VAV system that was modeled by using polynomial models of both systems. This improved the energy efficiency of the combined set of systems by 3% in the winter and 12% in the summer. Kim et al. (2016) also used a genetic algorithm to identify optimal setpoints for polynomial models of a building served by a VRF system and a DOAS system, and found that these setpoints were able to reduce the energy consumption by 20%. Finally, the present work extends the efforts described by Laughman et al. (2017), who studied the behavior of a combined HVAC system that combined a single evaporator vapor-compression cycle and a dedicated outdoor air system (DOAS), and which demonstrated energy savings of approximately 15% through setpoint optimization.

Equation-based, object-oriented languages for physical system modeling, such as Modelica (Modelica Association, 2017), represent an important enabling technology for efficiently and accurately describing the dynamic behavior of buildings with multiple interacting HVAC systems. The equation-based framework of such languages allows a modeler to create physically accurate desriptions of individual systems, and then couple these individual system models together to form a model of the overall system. These physics-based models have significant advantages over correlation-based or data-based models, as the model behavior can often be extrapolated beyond the calibrated data much more accurately. Because the system is represented by a graph-based structure of the underlying equations, these models can also be used for control system design and analysis, such as for the creation of linearized system models at specified operating points. The object orientation of these languages also makes it possible for the modeler to create multiple system models with a common interface that can be easily modified to perform trade studies and analyze the system dynamics; without this object orientation, each system model may have to be created from scratch, potentially introducing incompatible modeling assumptions and other errors.

In this work, we present a case study in using Modelica to implement a model-based process to design the HVAC system architecture and controls for a multi-zone building. The base system includes a split ductless air-conditioning system to provide cooling to all four rooms of a building, and we create models of three different ventilation systems that provide outdoor air for each of the spaces: a fan-only system, an energy recovery ventilation system (ERV), and a dedicated outdoor air system (DOAS). Each of these subsystems (building, air-conditioning system, ventilation system) is represented by a high-order system model, and these system models are interconnected to form a description of the heterogeneous building dynamics. We analyze the overall system dynamics to design the detailed equipment-level control systems to meet a set of performance criteria, and then run the full nonlinear system model with the closed-loop control to explore the differences in performance for all three system architectures.

This paper has a relatively simple structure. In Section 2, we describe the models for the variety of systems used in

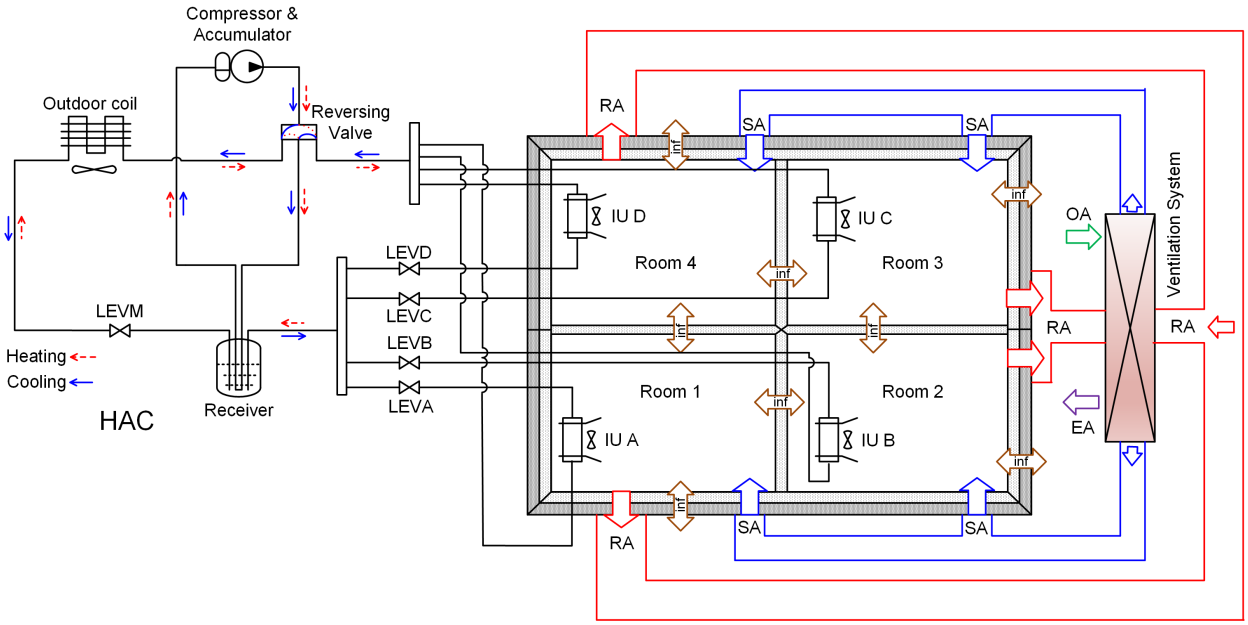

Figure 1: Building with four conditioned zones served by both vapor-compression air-conditioning and ventilation systems.

this work. This includes the model of the multi-zone split ductless system, the models for the individual ventilation systems, and the dynamic model of the building. We then use the resulting system models to analyze the coupled dynamics for the conditioned building in Section 3, and design control systems for the HVAC system that meet temperature and comfort requirements. These controlled systems are then used in Section 4 to run a set of simulations of the overall building to compare the performance of all three HVAC system architectures. A brief set of summarizing and concluding remarks is offered in Section 5.

2. MODELS

As briefly described in Section 1, this paper uses physics-based models to examine the dynamic behavior of a building with both cooling and ventilation systems under closed-loop control. The building with its space conditioning systems is illustrated from a top-down perspective in Figure 1, and has four conditioned zones and a single attic zone above all of the occupied spaces. Each of these spaces included air infiltration at a fixed flow rate, denoted *inf* in the figure, between adjacent zones, the attic, and the ambient environment. The air-conditioning system consists of a variable capacity vapor-compression system with a heat exchanger (HEX) located in each conditioned indoor space. This system includes a variable speed compressor, variable speed fans for both the condensing and evaporating heat exchangers, and linear expansion valves (LEVs) that regulate the flow of refrigerant through each indoor HEX. The refrigerant cycle also incorporates a high-side receiver and an auxiliary expansion valve (LEVM) at the outlet of the condensing HEX to manage the refrigerant distribution between heating and cooling operation, though the system is only operated in cooling mode in this study.

This base structure of the building with a cooling system is extended to construct three related models, each of which includes a different ventilation system. The first ventilation system consists solely of supply and return air fans, while the second system includes an ERV based upon enthalpy exchange between the supply air (SA) and return air (RA) streams as well as both fans. The third ventilation system studied is a DOAS that incorporates a deep cooling HEX to cool and dehumidify the inlet supply air, as well as a reheat coil that uses some of the condensing energy to reheat the supply air so that it is closer to the desired indoor air temperature. Modelica's object orientation was essential to this work as a system model was created with an abstract ventilation system, and the three different ventilation systems could replace the abstract system model in turn with almost complete code reuse to enable a direct trade study.

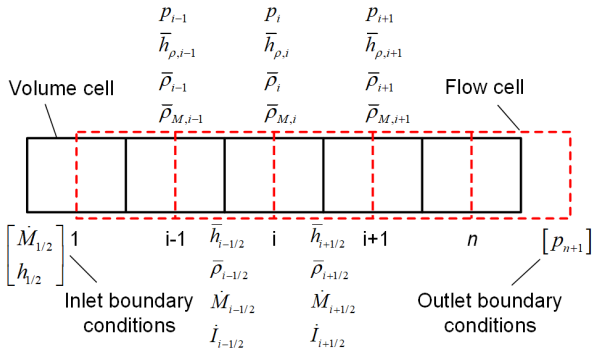

Figure 2: Finite volume discretization of refrigerant pipe.

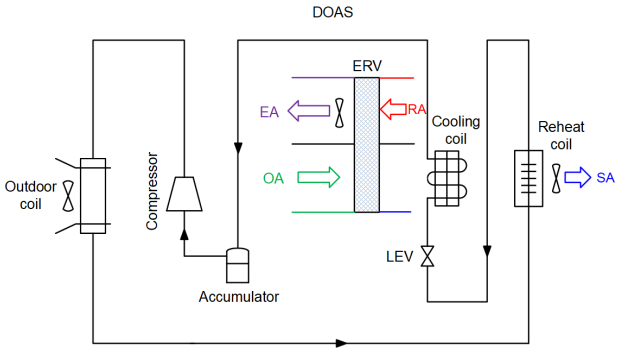

Figure 3: Structure of dedicated outdoor air system.

Because many of the systems used in this work are constructed from similar components, we first describe the physics-based models used to create the component objects, and then discuss the construction of the system models from this set of components. As many of these different system models have been described at length in previous publications, we emphasize only the details of these models needed to provide sufficient context for this paper.

2.1 Component Models

The temporal behavior of the vapor compression cycle is dominated by the heat exchangers over the time scales of seconds to days, so the system models in this work used dynamic models of the HEXs and receiver and static (algebraic) models of the compressor and expansion valves. The inclusion of long pipe lengths to describe the spans between the condensing HEX and the indoor HEXs, as well as the need to describe experimentally observed behavior of the HEXs, motivated the use of finite volume models (Li et al., 2014) for the refrigerant pipes. We assume 1-D flow for the refrigerant so that properties only vary along the length of the pipes; we also assume that the refrigerant can be described as a Newtonian fluid, negligible viscous dissipation and axial heat conduction in the direction of flow, negligible contributions to the energy equation from the kinetic and potential energy of the refrigerant, negligible dynamic pressure waves in the momentum equation, and thermodynamic equilibrium in each volume for which the refrigerant is in the two-phase region.

Under these assumptions, the partial differential equations describing the conservation of mass, momentum, and energy (Levy, 1999) for the refrigerant can be spatially discretized to construct a set of finite volume models. A staggered grid scheme, illustrated in Figure 2, is used to avoid nonphysical pressure variations caused by numerical artifacts by decoupling the mass and energy equations computed for the volume cells (represented by the black solid boundary) from the momentum equations computed for the flow cells (represented by the red dashed boundary). Integration of these equations across these cells, as well as the use of the upwind difference method to approximate refrigerant properties for the convection-dominated flows from this application, results in a set of ordinary differential equations describing the conservation equations, as given in Equations 1, 2, and 3.

$$A_c \Delta z \left(\frac{\partial \bar{\rho}_i}{\partial p_i} \frac{\mathrm{d}p_i}{\mathrm{d}t} + \frac{\partial \bar{\rho}_i}{\partial \bar{h}_{\rho,i}} \frac{\mathrm{d}\bar{h}_{\rho,i}}{\mathrm{d}t} \right) = \dot{M}_{i-1/2} - \dot{M}_{i+1/2}, \tag{1}$$

$$\Delta z \frac{\mathrm{d}\dot{M}_{i+1/2}}{\mathrm{d}t} = \dot{I}_i - \dot{I}_{i+1} - A_c (p_{i+1} - p_i) - P \Delta z \bar{\tau}_{w,i+1/2}, \tag{2}$$

$$A_c \Delta z \left(\bar{\rho}_i \frac{\mathrm{d}\bar{h}_{\rho,i}}{\mathrm{d}t} - \frac{\mathrm{d}p_i}{\mathrm{d}t} \right) = \dot{M}_{i-1/2} (h_{i-1/2} - \bar{h}_{\rho,i}) - \dot{M}_{i+1/2} (h_{i+1/2} - \bar{h}_{\rho,i}) + P \Delta z q''_i, \tag{3}$$

where $\bar{\rho}_M$ represents the momentum density, $\bar{h}_\rho$ and $\bar{h}$ signify the the density-weighted and flow-weighted specific enthalpies, the wall shear stress $\bar{\tau} = \frac{1}{2} f \bar{\rho} u |u|$ and f is the Fanning friction factor, and P is the circumference of the flow channel. These symbols with overbars represent average quantities in each cell. Pressure p and density-weighted specific enthalpy $\bar{h}_\rho$ are used as dynamic states in these models.

A set of simplified closure relations for the frictional pressure drop and the refrigerant-side heat transfer coefficients

were used because many correlations from the literature have poor numerical properties that make them unsuitable for inclusion in a dynamic simulation. The frictional pressure drop was expressed as $p/\dot{M}^2 = K\left(\Delta p_0/\dot{M}_0^2\right)$, where the Colebrook correlation for the single-phase friction factor where the Friedel correlation for two-phase multipliers were used to determine the nominal values of K, Δp_0, and $\dot{M}_0$. Simplified heat transfer relations for each phase were also used in which the heat transfer coefficient for each phase was only dependent upon the refrigerant mass flow rate, and the smooth transition between the phases was enforced via trigonometric interpolation. The constants used for these simplified heat transfer correlations were obtained from the Gnielinski correlation for single-phase fluids, the Dobson correlation for condensing flows, and the Gungor-Winterton correlation for evaporating flows.

A multicomponent moist-air model was used for the air-side of this work, in which both the dry air and the water vapor were described by ideal gas equations. The mass and energy conservation equations used to describe the heat transfer from the outer surface of the tubes to the air reflected this multicomponent model, as described by Equation 5, where the mass transfer coefficient was given by a modified Lewis correlation.

$$\dot{m}_{air} c_{p,air} \frac{dT_{air}}{dy} \Delta y = \alpha_{air} \left(A_{o,tube} + \eta_{fin} A_{o,fin}\right) \left(T_w - T_{air}\right) \tag{4}$$

$$\dot{m}_{air} \frac{d\omega_{air}}{dy} \Delta y = \alpha_m \left(A_{o,tube} + \eta_{fin} A_{o,fin}\right) \min\left(0, \omega_{water,sat} - \omega_{air}\right) \tag{5}$$

A simple isenthalpic model of the electronic expansion valve was also used, as described by a standard orifice flow equation

$$\dot{m} = C_v a_v \sqrt{\rho_{in} \Delta P}, \tag{6}$$

where the mass flow rate is regularized in the neighborhood of zero flow to prevent the derivative of the mass flow rate from tending toward infinity. The flow coefficient C_v is generally determined via calibration against experimental data, while the flow area a_v represents the control authority over the orifice size.

All cycle models in this work included a variable-speed high-side rotary compressor, in which the motor is cooled by the high-pressure refrigerant exiting from the compression mechanism. Due to the complex nature of the heat transfer and fluid flow through the compressor, we used simplified 1-D models of this component to parsimoniously describe the system. The behavior of the compressor was described by relating the volumetric efficiency η_v and isentropic efficiency η_{is} to the suction pressure P_{suc}, discharge pressure P_{dis}, and compressor frequency f, as given by

$$\eta_v = \frac{\dot{m}_{comp}}{\rho_{suc} V f} \tag{7}$$

$$\eta_{is} = \frac{h_{dis,isen} - h_{suc}}{h_{dis} - h_{suc}}. \tag{8}$$

The compressor power consumption $\dot{W}$ was also related to the compressor speed and the ratio of inlet and outlet pressures, i.e., $\dot{W}(P_{rat}, \omega)$. The coefficients used for the functional forms of η_v, η_{is}, and $\dot{W}$ were derived from experimental data, and the expressions are provided in Laughman et al. (2017).

Standard fan laws (ASHRAE, 2008) were used to describe the behavior of the heat exchanger fans, as well as the fans used in the DOAS system. According to such models, the volumetric flow rate was assumed to be directly proportional to the fan speed, while the power consumed by the fan was assumed to be proportional to the cube of the fan speed. These simple algebraic models were scaled by experimentally measured values of fan speed, flow rate, and power for a representative system; to minimize the error in these fits, linear and quadratic terms were also included in the power model to account for observed variations in the data.

While a detailed model of the heat and mass transfer between the air streams flowing through the energy recovery wheel would require significant effort, data from an experimental ERV indicated that this system can be accurately represented as having constant efficiencies for both heat and mass transfer. The amount of sensible heat transfer and the amount of water vapor exchange between the outdoor air stream and the exhaust air stream can thus be determined by

$$\dot{q}_s = \eta_s \min(\dot{m}_{OA} c_{p,a}, \dot{m}_{RA} c_{p,a})(T_{OA} - T_{RA}) \tag{9}$$

$$\dot{m}_w = \eta_w \min(\dot{m}_{OA}, \dot{m}_{RA})(\omega_{OA} - \omega_{RA}). \tag{10}$$

VRF Parameter	Value
Refrigerant	R410A
Total refrigerant mass (kg)	4.51
OU HEX tube diameter (mm)	9.5
IU HEX tube diameter (mm)	7
OU HEX tube length (m)	0.77
IU HEX tube length (m)	0.63
OU HEX number of tubes	16
IU HEX number of tubes	16

DOAS Parameter	Value
Refrigerant	R410A
Total refrigerant mass (kg)	4.57
OU HEX tube diameter (mm)	8
CC HEX tube diameter (mm)	9.5
RH HEX tube diameter (mm)	9.5
OU HEX tube length (m)	2.1
CC HEX tube length (m)	0.89
RH HEX tube length (m)	0.89
OU HEX number of tubes	9
CC HEX number of tubes	10
RH HEX number of tubes	10

Table 1: Heat exchanger geometric parameters for HAC and DOAS.

2.2 System models

These component models were used in Modelica to assemble an air-source air-conditioning system model with a separate evaporator located in each indoor space, as illustrated in Figure 1 and briefly described here. As is the case in most vapor compression cycles, the discharge gas leaving the compressor first flows into the outdoor heat exchanger, where it condenses to a liquid. This condensed refrigerant then passes through a first expansion valve (LEVM) and into a high-side receiver, after which it splits into a manifold that connects to each of the four indoor units. The refrigerant in each individual line then is further expanded through an additional expansion valve, which typically has a much smaller orifice size than LEVM, and then flows through adiabatic refrigerant pipes that are between 11 and 13 meters long. The refrigerant in each line then enters the indoor heat exchanger, where it evaporates and returns to the outdoor unit through another set of long pipes to a manifold that connects to the suction port of the compressor. Standard tube-fin heat exchangers were used for both the condenser and evaporators, as well as a rotary compressor and electronic expansion valves with a nearly linear response (LEV). Further details for the multi-zone vapor-compression system model are provided in Qiao et al. (2017).

While the DOAS system was constructed from the same underlying component models as the air-conditioning system model, the system configuration is quite different due to the presence of the reheat coil. The system architecture of the DOAS system is illustated in Figure 3. This system effectively splits the condensing heat exchanger into two parts, so that the high-pressure hot discharge gas leaving compressor is first partially cooled as it travels through the outdoor heat exchanger, and then continues to condense in the reheat coil. The subcooled liquid leaving the reheat coil is then expanded across the expansion valve LEV, after which it evaporates and returns to the suction port of the compressor. This coil configuration allows the cooling coil to first cool and dehumidify the hot, humid outdoor air, after which the ventilation air is reheated using the condenser heat to a temperature close to that of the room. Since we assume that the building is tight, the speeds of the supply air fan and the return air fan are equal.

A number of geometric and fluid parameters were required to configure both the air-source air-conditioner and the DOAS; particularly important quantities are provided in Table 1. Each indoor unit multi-zone system had a nominal cooling capacity of 1136 W sensible and 856 W latent at a compressor frequency of 55 Hz, with 2.93 °C of condenser subcooling when each indoor zone was at 23.5 °C and 4.6 °C of superheating in each evaporator when the ambient environment was at 27.2 °C. In comparison, the DOAS cooling coil had a nominal sensible capacity of 2297 W and latent capacity of 1663 W, while the reheat coil had a capacity of 486 W at a compressor frequency of 25 Hz. There were 18.9 °C of subcooling in the reheat coil, and 10 °C of superheating in the cooling coil at the ambient conditions of 27.2 °C and a relative humidity of 72%.

The models of the ERV and the fan-only ventilation system are much simpler than that of the DOAS, and can be generally understood by considering Figure 3 with the removal of the vapor compression cycle. Both the supply air fan and the exhaust air fan were identical, so that they each provided the same flow rate at the same speed. The heat transfer efficiency of the ERV was set to 0.65, while the mass transfer efficiency was set to 0.6.

2.3 Building Model

Unlike the cycle models used in this work, the building models were based upon the open-source Modelica Buildings library (Wetter et al., 2014), an extensive and well-tested library of components for the construction of dynamic building and building system models. Modelica is a powerful tool in this respect: models from different libraries can be coupled together, as long as the semantics of their connectors are satisfied, without requiring the engineering effort that would otherwise be required to ensure the correct computational flow for a simulation. In addition, the growing size of the Modelica community is associated with an increasing number of high-quality publicly-available model libraries, such as those organized under IBPSA Project 1, which can be leveraged to accelerate model-based research and development efforts.

The room models from the Buildings library are based on the physics-based behavior of the fundamental materials and components commonly used in the building construction industry. These individual materials are parameterized by fundamental properties like thickness, thermal conductivity, and density, and can be combined and assembled into multi-layer constructions. The accuracy of the multi-layer models is ensured by automating the discretization of the partial differential equations representing heat transfer in the materials by using the Fourier number to ensure that the time constants of each volume are approximately equal (Wetter, 2006). Similarly, the zone air model is a mixed air single-node model with one bulk air temperature that interacts with all of the radiative surfaces and thermal loads in the room, where the zone is assumed to have convective, radiative, and latent gains specified on a per area basis. The radiative heat transfer representing the solar heat gains and the infrared heat transfer between the interior surfaces of the room are also described by characterizing the absorptivity and emissivity of each surface, which is used with a set of simplified view factors between the surfaces in the room as an approximation to avoid the complexity of incorporating the detailed room geometries.

The specific building construction used in this work is shown schematically in Figure 1, and is based on the U.S. Department of Energy small commercial office building reference model (Deru et al., 2011); the main difference between the models is that the original U.S. DOE model also includes a core zone with no exterior surfaces, whereas the building model used here does not include this core zone. The four occupied zones in this building are oriented in the compass directions, and there is an additional attic zone that is connected to all of the occupied zones. As illustrated in the figure, each zone is assumed to have a leakage area between rooms of 0.01 m^2, and we also assume an infiltration flow rate from the ambient environment of 3.02×10^{-4} m^3/s per unit area for the exterior. This building is constructed on a 0.1 meter thick concrete slab, with a constant soil temperature of 21 °C. The convective heat transfer coefficients for the zones are 3 W/m^2K for the interior and $10 W/m^2K$ on the exterior, while the surfaces were assumed to have an absorptivity of 0.9. This building was located in Atlanta, GA, USA, and the corresponding TMY3 weather file was used to drive the model with realistic solar and thermal boundary conditions to understand the detailed room thermal dynamics. Each space was assumed to contain 8 W/m^2 of both convective and radiant load, and 4 W/m^2, which is roughly equivalent to 8 occupants that impose 70 W sensible load and 30 W latent load, as well as 400 W of equipment load. The total ventilation rate is 500 cfm, which corresponds to 125 cfm per space, which is above the 80 cfm minimum recommended fresh air ventilation rate prescribed by ASHRAE standard 62.1.

One technical concern that emerged in this work is that the structure of the moist air model had a significant influence on simulation time. Rather than use a full moist air model, we used a simplified air model that decoupled the pressure and temperature of the medium and resulted in much smaller sets of nonlinear equation blocks in the flattened model, which was accompanied by a corresponding increase in the simulation speed and a marginal decrease in accuracy. This was implemented by formulating the mass in each lumped air volume so that it was dependent only on the pressure, e.g., $m_{air} = V_{room}\rho_{STP}\left(p_{air}/p_{STP}\right)$.

3. CONTROLS

We designed the feedback control system illustrated in Figure 4 for the integrated VRF and DOAS systems. The architecture is decentralized: compensator K_V actuates the VRF, while K_D actuates the DOAS. However, each must be designed considering the coupled system. In this diagram, the input vector u_{VRF} includes the VRF compressor speed f_V, the four electronically actuated valves LEV_i, and the outdoor fan speed. The input vector u_{DOAS} includes the DOAS compressor speed f_D, its electronically actuated expansion valve $LEV3$, the outdoor fan speed, and the supply air fan speed. The disturbances d include the outdoor weather conditions (temperature, relative humidity, radiative terms, wind speed and direction) and indoor heat loads (sensible, latent, and radiative) for each zone. The arrows in

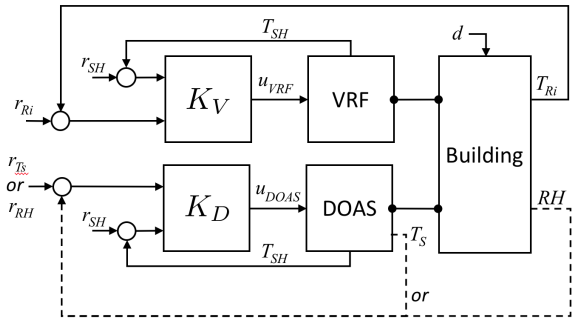

Figure 4: Block diagram of the control system.

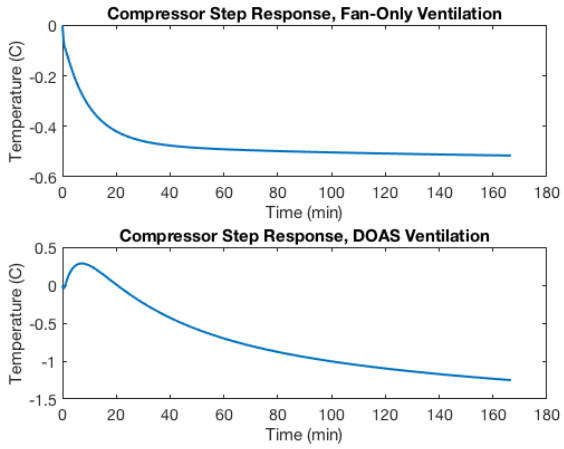

Figure 5: Step response of the air-conditioner compressor speed.

Figure 4 denote a causal relationship, while the lines with dots denote an acausal coupling. In particular, the presence of the DOAS system changes the dynamic behavior of the VRF system through the building.

The compensators K_V and K_D are designed using multivariable frequency domain methods, using a linearized and reduced-order model that is computed from the coupled VRF-DOAS-building Modelica model. The process used to generate the control-oriented model begins by simulating the Modelica model to a representative steady-state operating condition, and then computing a linearization. Importantly, Modelica and its supporting compilers compute this Jacobian symbolically, resulting in a sparse, high-order "raw" linearization. This integrated VRF-DOAS-building model has more than 1000 states, is more than 99% sparse, and has time scale separation of 10 orders of magnitude, making it exceptionally stiff and ill-conditioned. However, it can be reduced through a careful sequence of symbolic manipulations, modal decompositions, conventional Hankel norm truncations and singular perturbations, giving a low-order model that is numerically well conditioned, dense, low-order, and useful for control design. The capability of Modelica and its associated tools to compute reliably the raw linearization is an important advantage over other simulation tools.

The compensator K_V uses a cascade design, with inner feedback loops closed on the measured superheat of each indoor unit, and outer loops closed on the individual room temperatures, driving the inner loops and the compressor frequency. In addition, the indoor unit with the minimum value of superheat is selected for feedback. This ensures that the five actuators drive five signals (room temperatures and the minimum superheat) to their reference with integral action. When the system is operating with the fan-only ventilation or ERV, the design is a straight-forward application of multivariable feedback control, provides a high degree of robustness, good transient response and disturbance rejection, and the desired steady-state behavior. Anti-windup and some degree of constraint enforcement is relatively straightforward to realize in this design, but beyond the scope of this paper.

The compensator K_D consists of two feedback loops. The measured evaporator superheat is fed back through a PI-type compensator to actuate LEV, while either the supply air temperature T_S or the average building relative humidity RH is fed back to drive the compressor. Both designs will drive the system to a stable steady-state with good transient response and disturbance rejection. However, the building dynamics make the RH feedback considerably slower and potentially less robust, providing a lower robustness margin. T_S feedback is often preferred in practice, and is used in the simulations that follow.

It is interesting to note that the presence of the DOAS affects the VRF cycle dynamics. In Figure 5, we compare a scaled, open-loop step response from the VRF compressor speed f_v to one of the room temperatures T_{Ri}. The top plot shows the response with fan-only ventilation, and is probably what would be expected: there is a minimum-phase, approximately first-order response. The bottom plot shows the same step response when the DOAS is used; the VRF and DOAS interact dynamically in non-intuitive ways. In this case, the response of the room air temperature to the compressor step is non-minimum phase. This behavior imposes limits on the magnitude of the feedback gains used

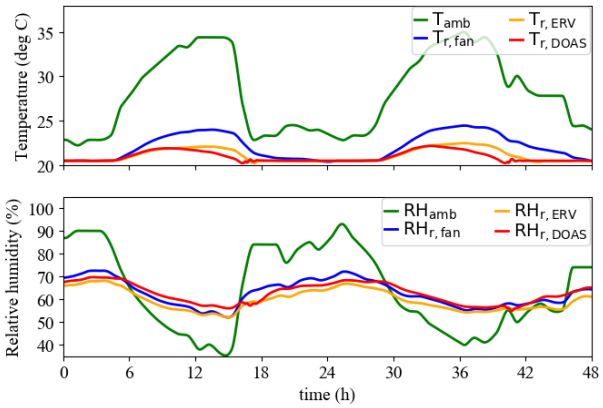

Figure 6: Ambient and room temperatures and humidities over 2 days for different ventilation systems.

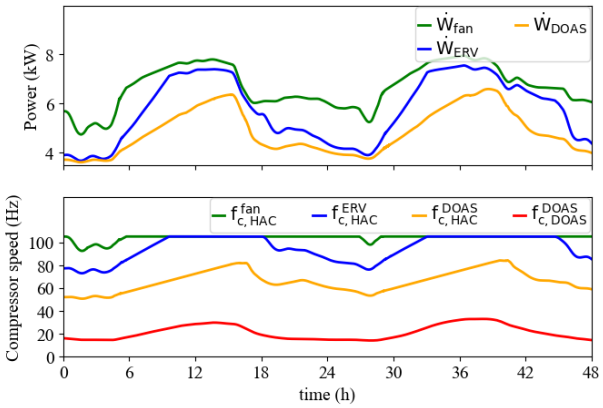

Figure 7: System power consumption and compressor speeds over 2 days for different ventilation systems.

by the VRF. Fortunately, the response from the VRF LEV_i is not similarly affected, so that K_V can be designed to have good robustness margins in spite of this non-minimum phase characteristic. Nevertheless, this effect must be quantified and included when designing the control system.

4. RESULTS

The models and controllers described Sections 2 and 3 were assembled into an overall system model and simulated over two days to study the differences in the system performance for the variety of ventilation system configurations. For all of these three scenarios, the supply air temperature setpoint was 16.9 °C, while the room air temperature setpoints were set to 20.5 °C, and the ventilation rates were constant. These simulations were performed on a laptop with an Intel i7 processor with 32 Gb of RAM using the Dymola 2018 FD01 compiler, and the differential algebraic equations were integrated with the DASSL solver with the tolerance set to 10^{-5}. Because of the complexity of these systems, the full models were very large; the flattened model with the multi-zone air-conditioner, the DOAS, and the building had 52807 equations and variables with 1063 states. The stiffness of the set of DAEs and the time-varying solar excitation also made the simulation of these models quite time consuming, with the average simulations requiring approximately 15.5 hours to describe 2 weeks of behavior.

Figures 6 and 7 illustrate a few salient variables that describe the behavior of the coupled systems. The room air temperature and relative humidity for one of the rooms are presented in Figure 6, as well as the ambient conditions on the days of July 11-12. While the room temperature in all of these cases varies to some extent, the fan-only ventilation system has much larger variations in the room temperature than either the ERV or DOAS ventilation systems because the large ambient infiltration rate presents a significant disturbance to the multi-zone air-conditioning system. Moreover, while the ERV and DOAS systems have similar room temperatures, the DOAS ventilation system has slightly smaller variations in room temperature than the ERV system due to its active control of the supply air temperature. In contrast, the relative humidities in the space for all three systems are relatively similar. The variation in the room relative humidity is larger for the fan-only system than for the ERV or the DOAS systems, as might be expected, but the differences are not large enough to be particularly significant. The small size of these humidity variations can be largely attributed to the high latent capacity of the individual evaporators for the multi-zone system with the fan-only and ERV ventilation, which assumption may not hold for all candidate multi-zone systems.

System	Energy consumption (kWh)
Fan ventilation	320.7
ERV ventilation	275.8
DOAS ventilation	232.7

Table 2: Total energy consumption over 2 days for alternate ventilation systems.

The behavior of the total system power and compressor speeds illustrated in Figure 7 also provide valuable information about the overall system performance. It is particularly interesting to note that the compressor speed for the fan-only system remains at its upper limit of 105 Hz during most of its operation, as the system does not have sufficient capacity to condition the load introduced by the supply air at the peak ambient conditions. This observation explains the large temperature fluctuations in the room air temperature for the fan-only system. While the ERV system remains at the the maximum compressor speed constraint for a shorter period of time than the fan-only system, the average compressor speed in this scenario is still much higher than either of the compressor speeds for the combined DOAS and multi-zone air-conditioning system. In particular, the multi-zone system never reaches this constraint over these two days, which results in improved transient system performance. This is also reflected in the estimates of the total energy consumption; the fan-only system has the highest total energy consumption (320.7 kWh), followed by the ERV (275.8 kWh) and finally the DOAS-based system (232.7 kWh). The benefits of the DOAS-based system are evident from consideration of this data, as it indicates that the HVAC system with the DOAS will be both more comfortable and consume signficantly less energy.

5. CONCLUSIONS

This work demonstrated an approach for comparing the behavior of different ventilation systems under closed-loop control that are coupled to both a controlled multi-zone air-conditioning system and a building. An accurate description of the interactions between these systems was found to be essential, as the power consumption of the overall system was strongly dependent upon these dynamics. Further work to refine this model-based process for performing trade studies and the integrated design of control architectures will be valuable in realizing the potential of high-performance buildings.

REFERENCES

ASHRAE (2008). *HVAC Systems and Equipment Handbook*. ASHRAE, Atlanta, GA.

Deru, M., Field, K., Studer, D., Benne, K., Griffith, B., Torcellini, P., Liu, B., Halverson, M., Winiarski, D., Rosenberg, M., Yazdanian, M., Huang, J., and Crawley, D. (2011). U.S. Department of Energy commercial reference building models of the national building stock. Technical report, National Renewable Energy Laboratory.

Karunakaran, R., Iniyan, S., and Goic, R. (2010). Energy efficient fuzzy based combined variable refrigerant volume and variable air volume air conditioning system for buildings. *Applied Energy*, 87:1158–1175.

Kim, W., Jeon, S., and Kim, Y. (2016). Model-based multi-objective optimal control of a VRF combined system with DOAS using genetic algorithm under heating conditions. *Energy*, 107:196–204.

Laughman, C., Qiao, H., Bortoff, S., and Burns, D. (2017). Simulation and optimization of integrated air-conditioning and ventilation systems. In *Proceedings of the 15th IBPSA Conference*, pages 1824–1833.

Levy, S. (1999). *Two-phase flow in complex systems*. New York: John Wiley & Sons.

Li, P., Qiao, H., Li, Y., Seem, J., Winkler, J., and Li, X. (2014). Recent advances in dynamic modeling of HVAC equipment. Part 1: Equipment modeling. *HVAC&R Research*, 20(1):136–149.

Modelica Association (2017). Modelica specification, Version 3.4.

Qiao, H., Laughman, C., Burns, D., and Bortoff, S. (2017). Dynamic characteristics of an R410A multi-split variable refrigerant flow air-conditioning system. In *12th IEA Heat Pump Conference*.

Wetter, M. (2006). Multizone building model for thermal building simulation in Modelica. In *International Modelica Conference*, pages 517–526.

Wetter, M., Zuo, W., Nouidui, T., and Pang, X. (2014). Modelica buildings library. *Journal of Building Performance Simulation*, 7(4):253–270.

Zhu, Y., Jin, X., Du, Z., and Fang, X. (2015). Online optimal control of variable refrigerant flow and variable air volume combined air conditioning system for energy saving. *Applied Thermal Engineering*, 80:87–96.